AMERICAN SOCIETY of
GENE & CELL
THERAPY

Long Non-coding RNA *PVT1* Promotes Cell Proliferation and Migration by Silencing *ANGPTL4* Expression in Cholangiocarcinoma

Yang Yu,[1,7] Mingjiong Zhang,[1,7] Jie Liu,[2,7] Boming Xu,[3] Jian Yang,[4] Ni Wang,[1] Shuai Yan,[5] Fei Wang,[1] Xuezhi He,[6] Guozhong Ji,[1] Quanpeng Li,[1] and Lin Miao[1]

[1]Medical Centre for Digestive Diseases, Second Affiliated Hospital, Nanjing Medical University, Nanjing, Jiangsu Province, People's Republic of China; [2]Reproduction Centre of Xuzhou Maternity and Child Health Care Hospital, Xuzhou, Jiangsu Province, People's Republic of China; [3]Department of Gastroenterology, Quanzhou First Hospital Affiliated to Fujian Medical University, Quanzhou, Fujian Province, People's Republic of China; [4]Department of Urology, Second Affiliated Hospital, Nanjing Medical University, Nanjing, Jiangsu Province, People's Republic of China; [5]Department of Oncology, Affiliated Jiangyin Hospital of Southeast University Medical College, Jiangyin, Jiangsu Province, People's Republic of China; [6]Research Centre for Bone and Stem Cells, Nanjing Medical University, Nanjing, Jiangsu Province, People's Republic of China

Cholangiocarcinoma (CCA) is the most common biliary tract malignancy, with a low survival rate and limited treatment options. Long non-coding RNAs (lncRNAs) have recently been verified to have significant regulatory functions in many kinds of human cancers. It was discovered in this study that the lncRNA *PVT1*, whose expression is significantly elevated in CCA, could be a molecular marker of CCA. Experiments indicated that *PVT1* knockdown greatly inhibited cell migration and proliferation *in vitro* and *in vivo*. According to RNA sequencing (RNA-seq) analysis, *PVT1* knockdown dramatically influenced target genes associated with cell angiogenesis, cell proliferation, and the apoptotic process. RNA immunoprecipitation (RIP) analysis demonstrated that, by binding to epigenetic modification complexes (PRC2), *PVT1* could adjust the histone methylation of the promoter of *ANGPTL4* (angiopoietin-like 4) and, thus, promote cell growth, migration, and apoptosis progression. The data verified the significant functions of *PVT1* in CCA oncogenesis, and they suggested that *PVT1* could be a target for CCA intervention.

INTRODUCTION

Cholangiocarcinoma (CCA), the most common biliary tract cancer, represents 3% of all gastrointestinal malignancies, and it is described as a malignancy originating from the ductal epithelial cells lining the intrahepatic and extrahepatic biliary ducts.[1] According to its anatomic origin, CCA is classified as intrahepatic (ICC), perihilar (pCCA), or distal (dCCA) CCA.[2] CCA is a destructive malignancy with an extremely poor general 5-year survival rate of less than 10%,[3] and patients have a median survival of 24 months after diagnosis, indicating that CCA has a poor prognosis.[4] Surgical resection and liver transplantation are possibly curative treatments for early stage CCA patients, and the median 5-year survival after R0 resection is approximately 30%;[5] however, because of the destructive malignancy of CCA, most patients already have advanced disease

at diagnosis.[3] Furthermore, patients with CCA have insensitivity to conventional chemotherapy or radiotherapy.[6] Therefore, there are no potentially curative clinical therapeutic interventions for CCA, and no targeted molecular therapies have been adopted for use in CCA.

Long non-coding RNAs (lncRNAs) represent enormous RNA families that are defined by a length of over 200 nt. lncRNAs have limited protein-coding potential and lack detectable open reading frames (ORFs), which are necessary for protein-coding potential.[7–11] Recently, lncRNAs have been demonstrated to play pivotal roles in many biological processes, such as cellular proliferation, development, and differentiation. lncRNAs can adjust gene expression in diverse biological functions by binding with transcription factors,[12] chromatin-modifying factors,[13,14] and heterogeneous nuclear ribonucleoproteins (hnRNPs);[15] lncRNAs can also act as regulators targeting the splicing, translation, or stability of host mRNAs through post-transcriptional mechanisms, or they can act as endogenous microRNA sponges to modulate microRNA targets.[16–18] It is noteworthy that the abnormal expression of lncRNAs has been proven in many cancers, such as CCA.[19–26]

Plasmacytoma variant translocation 1 (*PVT1*) localizes downstream of the *MYC* gene and maps to chromosome 8q24. *PVT1*

Correspondence: Lin Miao, Medical Centre for Digestive Diseases, Second Affiliated Hospital, Nanjing Medical University, 121 Jiangjiayuan, Nanjing 210011, Jiangsu Province, People's Republic of China.
E-mail: linmiao@njmu.edu.cn
Correspondence: Quanpeng Li, Medical Centre for Digestive Diseases, Second Affiliated Hospital, Nanjing Medical University, 121 Jiangjiayuan, Nanjing 210011, Jiangsu Province, People's Republic of China.
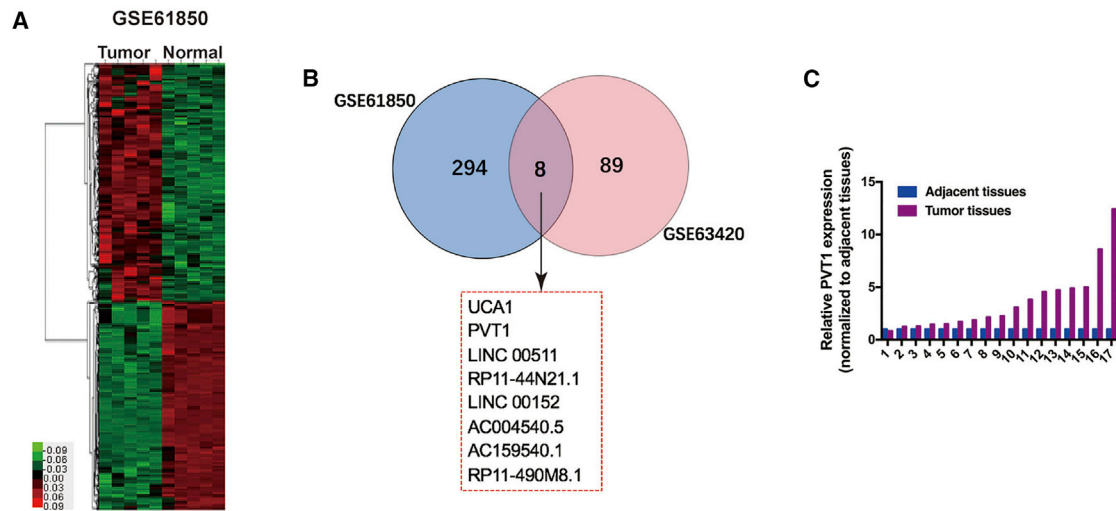**E-mail:** liquanpengxh@foxmail.com

Figure 1. The lncRNA *PVT1* Is Overexpressed in Cholangiocarcinoma Tissues

(A) Hierarchical clustering analysis of lncRNAs that were differentially expressed (fold change > 2; p < 0.05) in cholangiocarcinoma tissues and normal tissues. (B) Overlap of dysregulated lncRNAs in GEO datasets. (C) *PVT1* was detected in 17 pairs of CCA tissues by qRT-PCR. The levels of *PVT1* in CCA tissues were significantly higher than those in non-tumorous tissues.

specifically facilitates the invasive pathophysiology of ovarian cancer,[27] breast cancer,[28] and esophageal squamous cell carcinoma,[29] and overexpression of *PVT1* is an effective predictor of oncogenesis and overall survival in patients with multifarious cancers, including colorectal cancer[30] and gastric cancer.[31] However, the association between the abnormal expression and biological functions of *PVT1* in CCA and the underlying mechanisms remains undiscovered.

We discovered a CCA-specific upregulated lncRNA, *PVT1*, that displayed markedly elevated expression levels in CCA compared to normal tissues. The functional association between the underlying molecular mechanism and the effect of its overexpression in CCA was not determined.

RESULTS

PVT1 Is Upregulated in Human CCA Tissues

PVT1, situated at the chromosomal locus 8q24.21, encodes a transcript of 1,957 bp. To conduct a comprehensive characterization of aberrantly expressed lncRNAs in CCA, an analysis of GSE CCA and normal tissue microarray data was conducted; the results showed that *PVT1* expression is higher in tumor tissues than in ordinary tissues in the GEO: GSE61850 and GSE63420 datasets (Figures 1A and 1B). To verify this finding, *PVT1* expression in a cohort of 17 paired CCA tumors and ordinary tissues was detected with qRT-PCR, and the results confirmed that *PVT1* was markedly upregulated in carcinoma tissues (Figure 1C). However, the functional association and underlying molecular mechanism of *PVT1* and the effectors involved in its overexpression were not determined.

Knockdown of *PVT1* Inhibits CCA Cell Proliferation and Migration *In Vitro*

First, qRT-PCR was conducted to study the biological functional effects of *PVT1* dysregulation in CCA. As shown in Figure 2A, the qRT-PCR results showed that the expression of *PVT1* in the small interfering RNA (siRNA)-mediated knockdown group was significantly lower than that in the scrambled negative control siRNA (si-NC) group for the HuCCT1 and RBE cell lines. Colony formation was greatly decreased with knockdown of *PVT1* (Figure 2B). Additionally, CCK-8 assays revealed that knockdown of *PVT1* expression significantly reduced cell viability in both the HuCCT1 and RBE cell lines compared with that in the control cells (Figure 2C). Transwell assays showed that knockdown of *PVT1* dramatically repressed the migration of cells (Figure 2D).

Knockdown of *PVT1* Causes Apoptosis by Promoting Cell-Cycle Arrest *In Vitro*

To further study whether *PVT1* could affect apoptosis in CCA cell lines, flow cytometry was performed. The findings revealed that the HuCCT1 and RBE cell lines transfected with *PVT1* siRNA had higher apoptotic rates than did the control group (Figure 3A). Next, to determine whether the impacts of *PVT1* on CCA cell proliferation and migration were due to *PVT1*-mediated alterations in the progression of the cell cycle, we performed flow cytometry assays in both the HuCCT1 and RBE cell lines. The flow cytometry assays revealed that *PVT1* knockdown increased the proportion of cells in the G0/G1 phase and reduced the proportion of cells in the S and G2/M phases compared to the proportions in the control cells (Figure 3B). All the data suggested that *PVT1* could accelerate cell proliferation and migration by
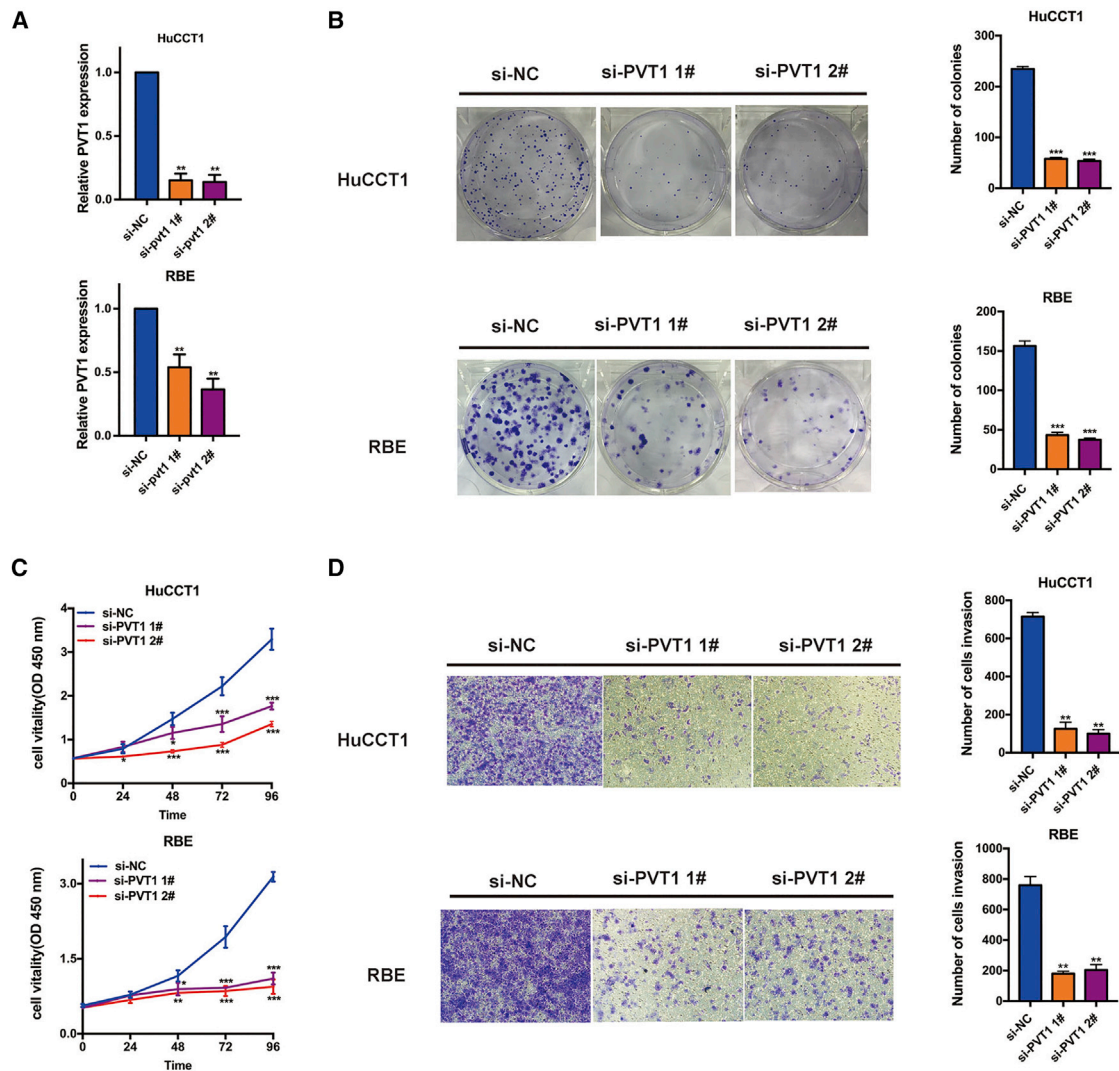
Figure 2. *PVT1* Promotes Cell Proliferation and Migration in Cholangiocarcinoma Cells

(A) qRT-PCR was used to determine the expression of *PVT1* after siRNA transfection in the HuCCT1 and RBE cell lines. (B) Colony formation assays were used to determine the colony-forming ability of si-*PVT1*-transfected cells. (C) CCK-8 assays were used to determine the viability of si-*PVT1*-transfected cholangiocarcinoma cells. (D) Transwell assays showed that *PVT1* knockdown inhibited cholangiocarcinoma cell migration. The error bars indicate the means ± SD. *p < 0.05, **p < 0.01, ***p < 0.001.

influencing cell cycle progression and inhibiting apoptosis in CCA cell lines.

Knockdown of *PVT1* Inhibits CCA Cell Tumorigenesis *In Vivo*

To confirm whether *PVT1* influences CCA tumorigenesis *in vivo*, HuCCT1 cells transfected with sh-*PVT1* or a control vector were injected into nude mice. At 16 days post-injection, the tumors established in the sh-*PVT1* group were dramatically smaller than those in the control group (Figures 4A and 4B). Correspondingly, the average tumor volumes and weights in the final experiment were markedly lower in the sh-*PVT1* group than in the control vector group (Figures 4C and 4D). These findings indicated that silencing *PVT1* could repress CCA tumor growth *in vivo*.

Related Target Genes of *PVT1* in CCA

To define the target mRNAs that could be regulated by *PVT1* in CCA, RNA transcriptome sequencing was performed after transfection with control siRNA or siRNAs against *PVT1*. Upon *PVT1* silencing, a set of 540 common mRNAs showed ≥1.5-fold increases in abundance, while 755 genes showed decreased abundance (≤1.5-fold). To prioritize the genes most related to *PVT1*, attention was paid to the genes that were the most highly expressed upon knockdown of *PVT1*. Interestingly, many well-known genes related to proliferation and migration (e.g., *ETV5*, *EREG*, *ENC1*, *ANGPTL4*, sprouty RTK signaling antagonist 4 [*SPRY4*], *GDF15*, and others) were included (Figure 5A; Table S2). Moreover, gene ontology analysis indicated that the most markedly overrepresented biological processes were
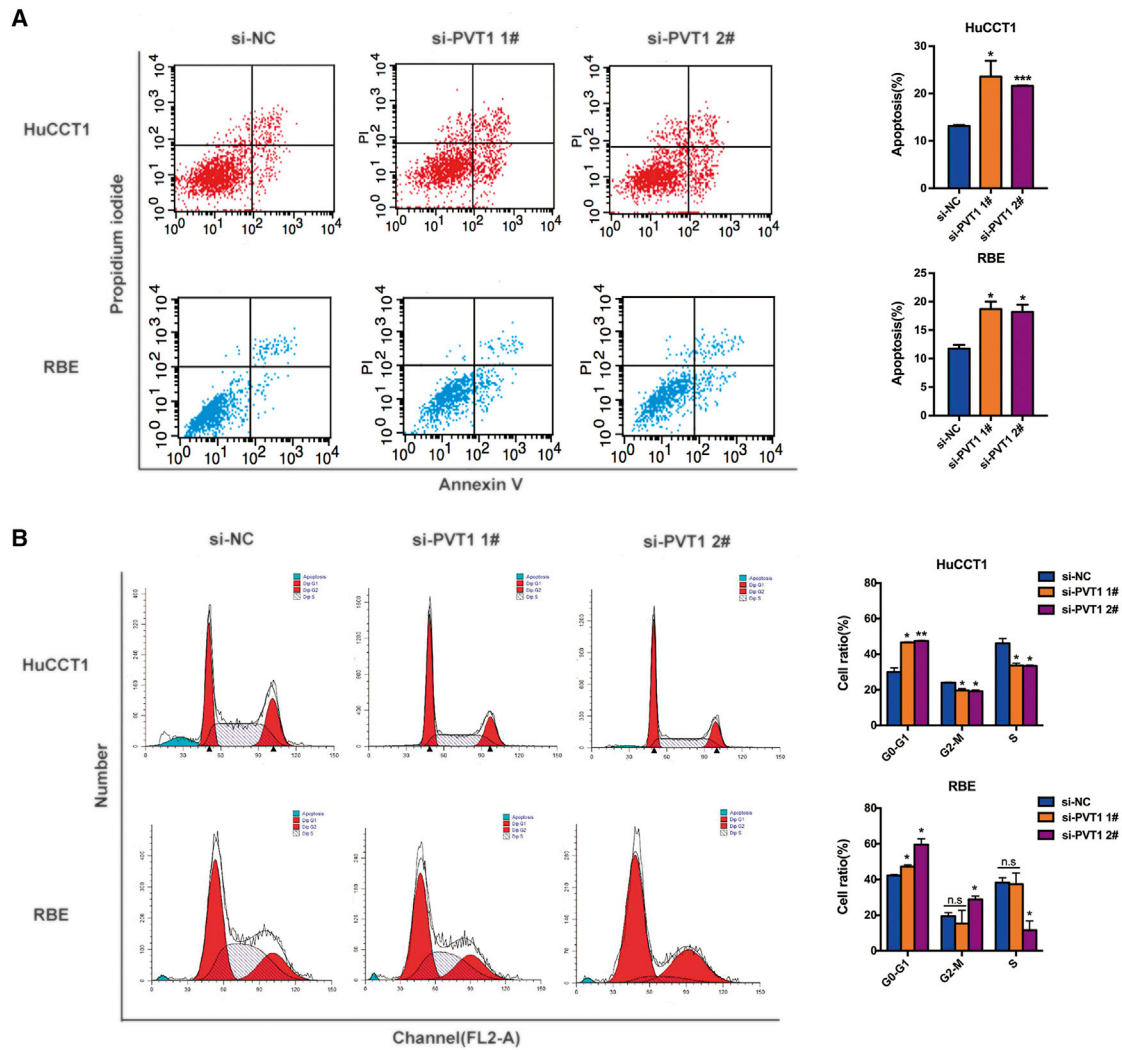
Figure 3. Knockdown of *PVT1* Causes Apoptosis by Promoting Cell-Cycle Arrest *In Vitro*

(A) Fluorescence-activated cell sorting (FACS) analysis of the effect of *PVT1* on apoptosis. (B) FACS analysis of the effect of *PVT1* on cell cycle progression. The error bars indicate the means ± SD. *$p < 0.05$, **$p < 0.01$, ***$p < 0.001$; ns, not significant.

pathways involved in angiogenesis, cell proliferation, and apoptosis progression (Figure 5B). Some of these genes were verified by qRT-PCR after knockdown (Figures 5C and 5D) and overexpression (Figure 5E) of *PVT1* in HuCCT1 and RBE cells, respectively.

PVT1 Binds with EZH2 to Coregulate Target Genes, Especially ANGPTL4

According to recent literature, many lncRNAs have been verified to cooperate with chromatin-modifying enzymes to accelerate epigenetic activation and, thus, silence target gene expression.[32] In particular, PRC2, a classic methyltransferase consisting of enhancer of zeste homolog 2 (EZH2), EED, and SUZ12 subunits, can serve as a catalyst not only in the dimethylation but also in the trimethylation of lysine residue 27 of histone 3 (H3K27me3), thus epigenetically repressing the expression of target genes.[33]

In our study, to investigate the mechanism of PVT1-mediated regulation, subcellular fractionation assays were first performed, which verified the localization of *PVT1* mainly in the nucleus (Figure 6A). Similarly, an RNA fluorescence *in situ* hybridization (FISH) assay showed that *PVT1* localized mainly in the nuclei of RBE cells (Figure 6B). In addition, the probability of interaction of EZH2 and *PVT1* was determined with an online tool (http://pridb.gdcb.iastate. edu/RPISeq/index.html), and the result showed that EZH2 could bind with *PVT1* well (random forest [RF] = 0.75, support vector machine [SVM] = 0.83) (Figure 6C). As revealed in Figure 6D, relative endogenous *PVT1* expression was amplified in the anti-EZH2 RNA immunoprecipitation (RIP) fraction compared to the immunoglobulin G (IgG) fraction in the HuCCT1 and RBE cell lines. Furthermore, simultaneous RNA FISH to detect *PVT1* and immunofluorescence for EZH2 showed nuclear co-localization mainly in HuCCT1 cells
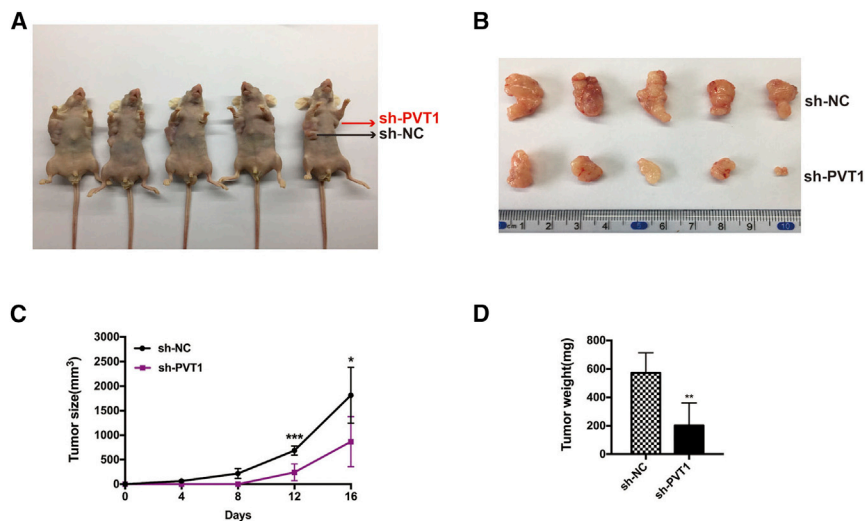
Figure 4. *PVT1* Regulates CCA Cell Proliferation *In Vivo*

(A) Tumors established with the mice in the scrambled control or sh-PVT1 group. (B) The size of tumors in the scrambled control or sh-PVT1 group. (C) After cell injection, the tumor volumes were calculated every 4 days. (D) The tumor weights are presented as the means ± SD. The error bars indicate the means ± SD. *p < 0.05, **p < 0.01, ***p < 0.001.

(Figure 6E). Together, these results confirmed that PVT1 could interact with EZH2.

We hypothesized that EZH2 could coregulate *PVT1*-mediated gene suppression by binding with *PVT1*. First, we investigated the expression of *PVT1*-suppressed genes in cells with *EZH2* knockdown or overexpression using qRT-PCR. The results showed that most of the *PVT1*-suppressed genes were upregulated by *EZH2* knockdown (Figure 6F) in the HuCCT1 and RBE cell lines. In contrast, decreased expression of *PVT1*-suppressed genes was observed upon overexpression of *EZH2* (Figure 6G). In addition, many studies have revealed that the included genes are influenced by hypermethylation of promoter loci in cancer.[34]

Subsequently, to assess the correlation between *EZH2* expression and the candidate target gene signature in CCA tissues, we analyzed the dataset GEO: GSE26566 (104 cancer tissue samples and 59 normal tissue samples) from the Molecular Signature Database, and correlation analysis revealed that *ANGPTL4* had a significantly negative correlation with *EZH2* in the GEO: GSE26566 dataset (Figure 6H). The protein level of ANGPTL4 was upregulated when *PVT1* or *EZH2* was knocked down (Figure 6I). In contrast, the protein level of ANGPTL4 was downregulated when *PVT1* or *EZH2* was overexpressed (Figure 6J). In summary, we elucidated one of the genes coregulated by *PVT1* and EZH2, angiopoietin-like 4 (*ANGPTL4*), which might be a tumor suppressor gene in CCA.

PVT1 Binds with EZH2 in the Nucleus and Epigenetically Silences *ANGPTL4*, Inhibiting Cell Proliferation and Migration in CCA Cell Lines

ANGPTL4, which is located on chromosome 19p13.2 and encodes a glycosylated, secreted protein with a C-terminal fibrinogen domain, can not only regulate glucose and lipid metabolism and insulin sensitivity but also serve as an apoptosis survival element for vascular endothelial cells, helping these cells avoid metastasis by preventing vascular

development and tumor cell invasion. In addition, it has been proven that hypermethylation of the *ANGPTL4* promoter region facilitates *ANGPTL4* transcriptional inactivation.[35]

First, to assess *ANGPTL4* expression in CCA tissues, we performed an analysis of the dataset GEO: GSE26566 (104 cancer tissues and 59 normal tissue samples), and we found that one of the candidate genes, *ANGPTL4*, was expressed at lower levels in CCA tissues than in normal tissues (Figure 7A). Subsequently, *ANGPTL4* expression was found to be lower in CCA tumor tissues than in neighboring tissues in an analysis of a cohort of 17 pairs of CCA tumor tissues and adjacent tissues using qRT-PCR (Figure 7B). Furthermore, overexpression of *ANGPTL4* could significantly suppress HuCCT1 and RBE proliferation and migration, and overexpression of *ANGPTL4* could partly reverse *PVT1*-induced growth and migration (Figures 7C–7F).

To further determine whether *PVT1* suppressed the expression of *ANGPTL4* by interacting with EZH2, chromatin immunoprecipitation (ChIP) analysis was carried out. ChIP assays revealed that knockdown of *PVT1* reduced EZH2 binding and H3K27me3 levels throughout the promoters of *ANGPTL4* (Figure 7G). In contrast, EZH2 binding and H3K27me3 levels increased throughout the promoters of *ANGPTL4* when *PVT1* was overexpressed (Figure 7H). These results confirmed that EZH2 could directly bind to the promoter region of *ANGPTL4* and then repress *ANGPTL4* expression directly by mediating H3K27me3 demethylation (Figure 7I).

Our results revealed that knockdown of *PVT1* reduced EZH2 binding and H3K27 trimethylation levels throughout the promoters of *ANGPTL4*, confirming that *ANGPTL4* is a target gene of *PVT1*. Our results demonstrated that *PVT1* promotes CCA malignancy by binding with EZH2 and then epigenetically repressing the expression of *ANGPTL4* in the nucleus.

DISCUSSION

Thus far, the newly identified lncRNAs have proven to be critical players in diverse human diseases, particularly in human cancers. The current study demonstrated that the expression of *PVT1* in CCA tissues was much higher than that in matched non-tumor
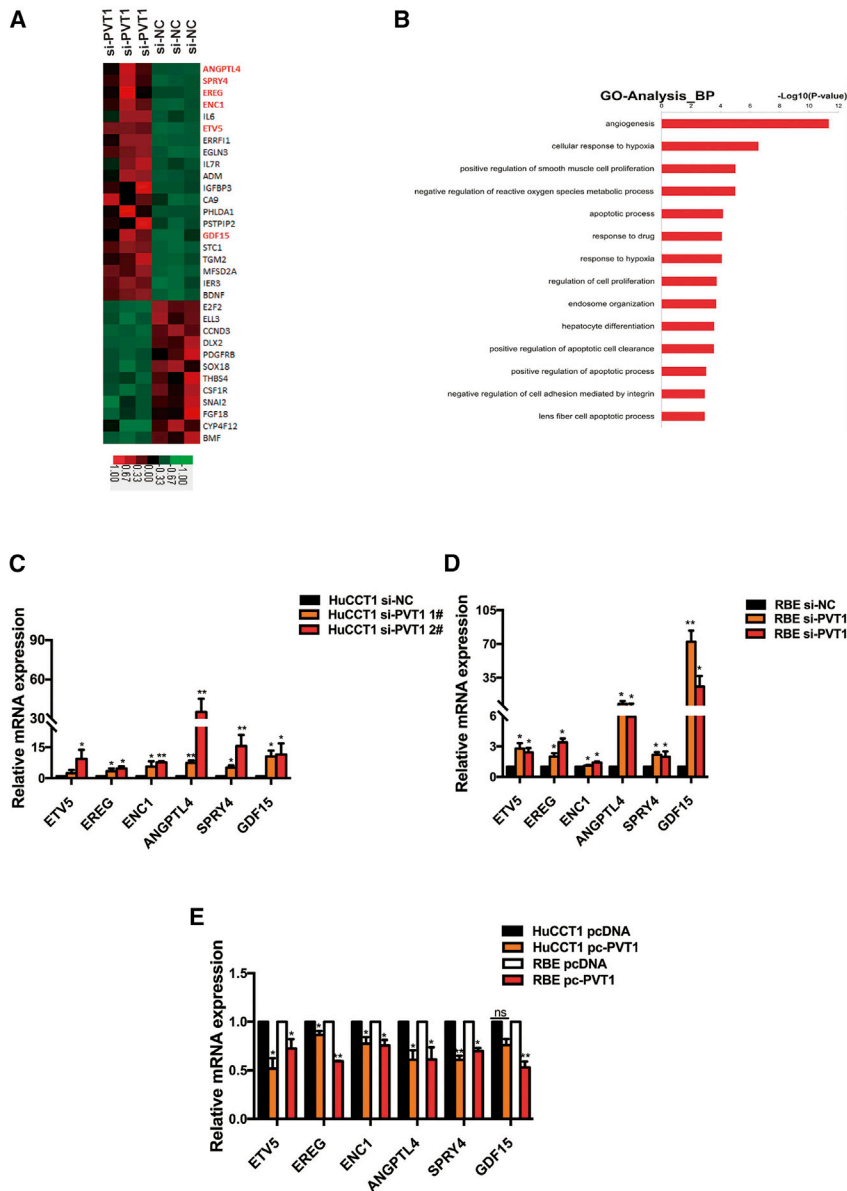
related to proliferation and migration, which was consistent with the prevention of proliferation and migration in the CCA cell line after *PVT1* knockdown. Recently, many lncRNAs have been verified to cooperate with chromatin-modifying enzymes to stimulate epigenetic activation and, thus, silence the expression of target genes.[32] For instance, the lncRNA *PVT1* can interact with EZH2, which is necessary for the repression of p15 and p16 in gastric cancer.[31] Moreover, lncRNAs can serve as scaffolds for protein complexes.[40–42] For example, the lncRNA *CCAT1* can act as a scaffold for double epigenetic modification complexes (the 5′ domain of *CCAT1* binds to PRC2 and the 3′ domain binds to SUV39H1), and then it can mediate histone methylation at the promoter locus of *SPRY4* in esophageal squamous cell carcinoma.[34] Our results showed that *PVT1* could bind with EZH2 to form a kind of histone methylation modification complex in the nucleus. Thus, a series of gene expression patterns can be regulated in CCA.

Previous studies have shown that *ANGPTL4* can act as a tumor suppressor gene in many types of cancers.[43] Nevertheless, the function of *ANGPTL4* in the tumorigenesis of CCA remains unknown. In addition, previous studies have verified that DNA methylation of the *ANGPTL4* promoter region leads to the inactivation of *ANGPTL4* transcription.[44] Our data revealed that histone methylation (H3K27me3) modulated by *PVT1* could facilitate the reduction in *ANGPTL4* expression in CCA cell lines. Taken together, our results demonstrated that *PVT1* binds with EZH2 and epigenetically silences *ANGPTL4* in the nucleus.

In summary, our study demonstrated the regulatory mechanism of *PVT1* in tumorigenesis. Through this mechanism, *PVT1* can promote the malignancy of CCA by epigenetically regulating the transcription

tissues. This finding elucidated the fact that *PVT1* might play a significant role in CCA malignancy. *PVT1* is upregulated in pancreatic cancer,[36] esophageal squamous cell carcinoma,[29] breast cancer,[37] hepatocellular carcinoma,[38] and gastric cancer,[39] and it has been found to promote the proliferation and invasion of cancer cells in many previous studies.

We discovered that silencing *PVT1* could inhibit CCA cell proliferation and migration *in vitro* and *in vivo*. Although *PVT1* has been claimed to have oncogenic functions in diverse kinds of cancer, the genes regulated by *PVT1* have not yet been discovered. Gene ontology analysis of the RNA sequencing (RNA-seq) results after *PVT1* knockdown revealed that the altered genes were especially
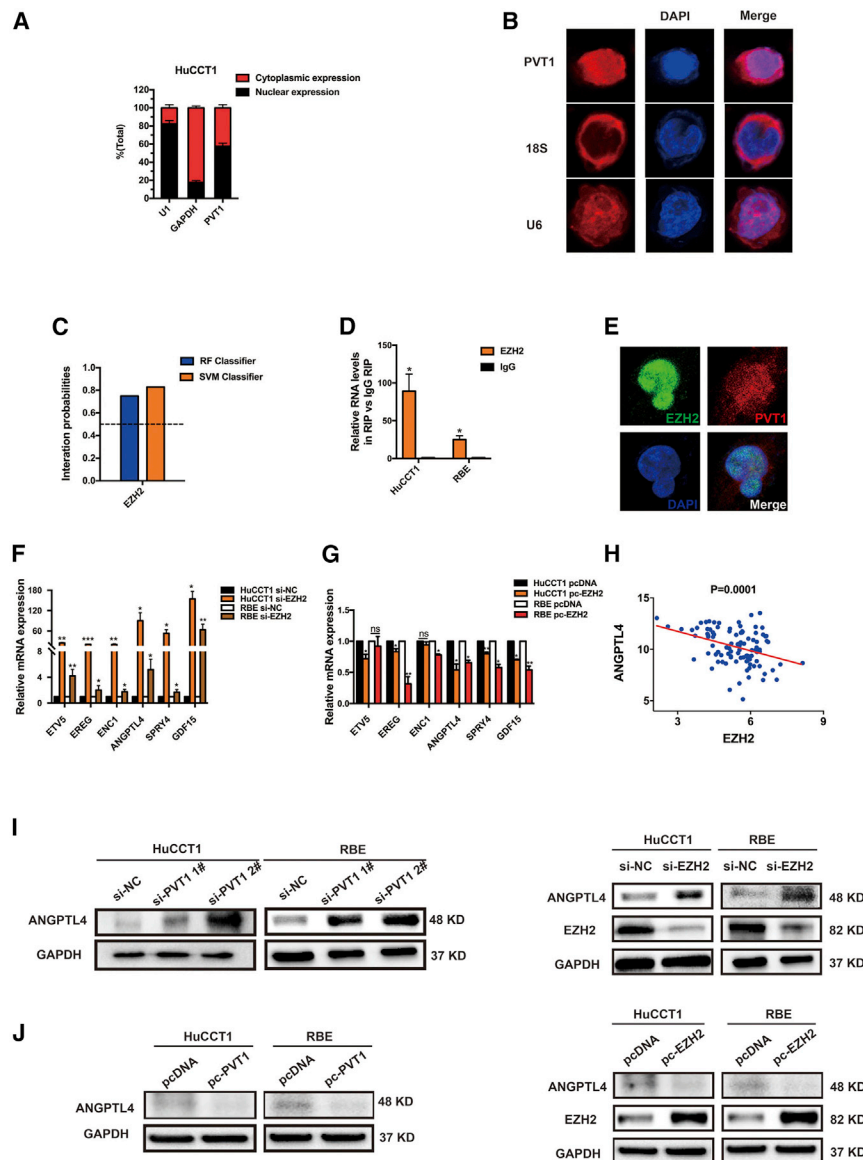
Figure 6. *PVT1* **Binds with EZH2 to Coregulate Target Genes, Especially** *ANGPTL4*

(A) After nuclear and cytosolic separation, RNA expression levels were measured by qRT-PCR. GAPDH was used as a cytosolic marker and U1 was used as a nuclear marker. (B) Fluorescent images of RBE cells treated with anti-*PVT1* (red), anti-*18S* (red), and anti-*U6* (red) RNA probes. DAPI staining is shown in blue. (C) The probability of interaction of EZH2 and *PVT1* was determined with an online tool (http://pridb.gdcb.iastate.edu/RPISeq/index.html). Predictions with probabilities >0.5 were considered positive. RPI-seq predictions are based on random forest (RF) or support vector machine (SVM). (D) An RIP experiment for EZH2 was performed, and the coprecipitated RNA was subjected to qRT-PCR for *PVT1*. (E) Expression and co-localization of EZH2 and *PVT1* in HuCCT1 cells. Representative fluorescent images show HuCCT1 cells treated with fluorescently labeled anti-EZH2 antibody (green) and anti-*PVT1* RNA (red). DAPI staining indicates the cell nuclei (blue). (F) Methylation-related genes were detected by qRT-PCR in the HuCCT1 and RBE cell lines after knockdown of *EZH2*. (G) Methylation-related genes were detected by qRT-PCR in the HuCCT1 and RBE cell lines after overexpression of *EZH2*. (H) The correlation between *EZH2* and *ANGPTL4* expression was detected by analyzing GEO: GSE26566 data. (I) The altered protein levels of ANGPTL4 were selectively confirmed by western blot analysis in cells with knockdown of *PVT1* or *EZH2*. (J) The altered protein levels of ANGPTL4 were selectively confirmed by western blotting in cells overexpressing *PVT1* or *EZH2*. The error bars indicate the means ± SD. *p < 0.05, **p < 0.01, ***p < 0.001; ns, not significant.

of *ANGPTL4* in the nucleus, thus facilitating cell survival and the metastasis of CCA. Our results suggest that *PVT1* could be a potential novel biomarker and a therapeutic target for CCA patients (Figure 7).

MATERIALS AND METHODS

Tissue Gathering and Ethics Statement

Altogether, 17 patients were analyzed in this research, all of whom underwent CCA resection at the Second Affiliated Hospital, Nanjing Medical University. All the specimens were instantly frozen in tubes with RNAlater preservation liquid after being removed, and they were kept in liquid nitrogen until the extraction of RNA. Our research was permitted by the Ethics Committee of Nanjing Medical University (Nanjing, Jiangsu, PRC), and written informed consent was obtained from every patient.

RNA Extraction and qRT-PCR Analyses

All RNA was obtained from cultured cells or specimens with TRIzol reagent (Invitrogen, Carlsbad, CA, USA). Then, for qRT-PCR, 1 μg RNA was reverse transcribed into cDNA with a reverse transcription kit (Takara, Tokyo, Japan). Real-time PCR analyses were carried out with SYBR Green (Takara, Tokyo, Japan). The findings were normalized to the expression of glyceraldehyde-3-phosphate dehydrogenase (GAPDH). The primer sequences are shown in Table S1.

Cell Culture

The CCA cell lines HuCCT1 and RBE were obtained from the Institute of Biochemistry and Cell Biology of the Chinese Academy of Sciences (Shanghai, China). All cell lines were maintained in DMEM (Life Technologies, Grand Island, NY, USA) containing 10% fetal bovine serum (FBS) (ScienCell, Carlsbad, CA, USA), 100 mg/mL streptomycin, and 100 U/mL penicillin (Invitrogen, Shanghai, China), in humidified air at 37°C with 5% CO_2.
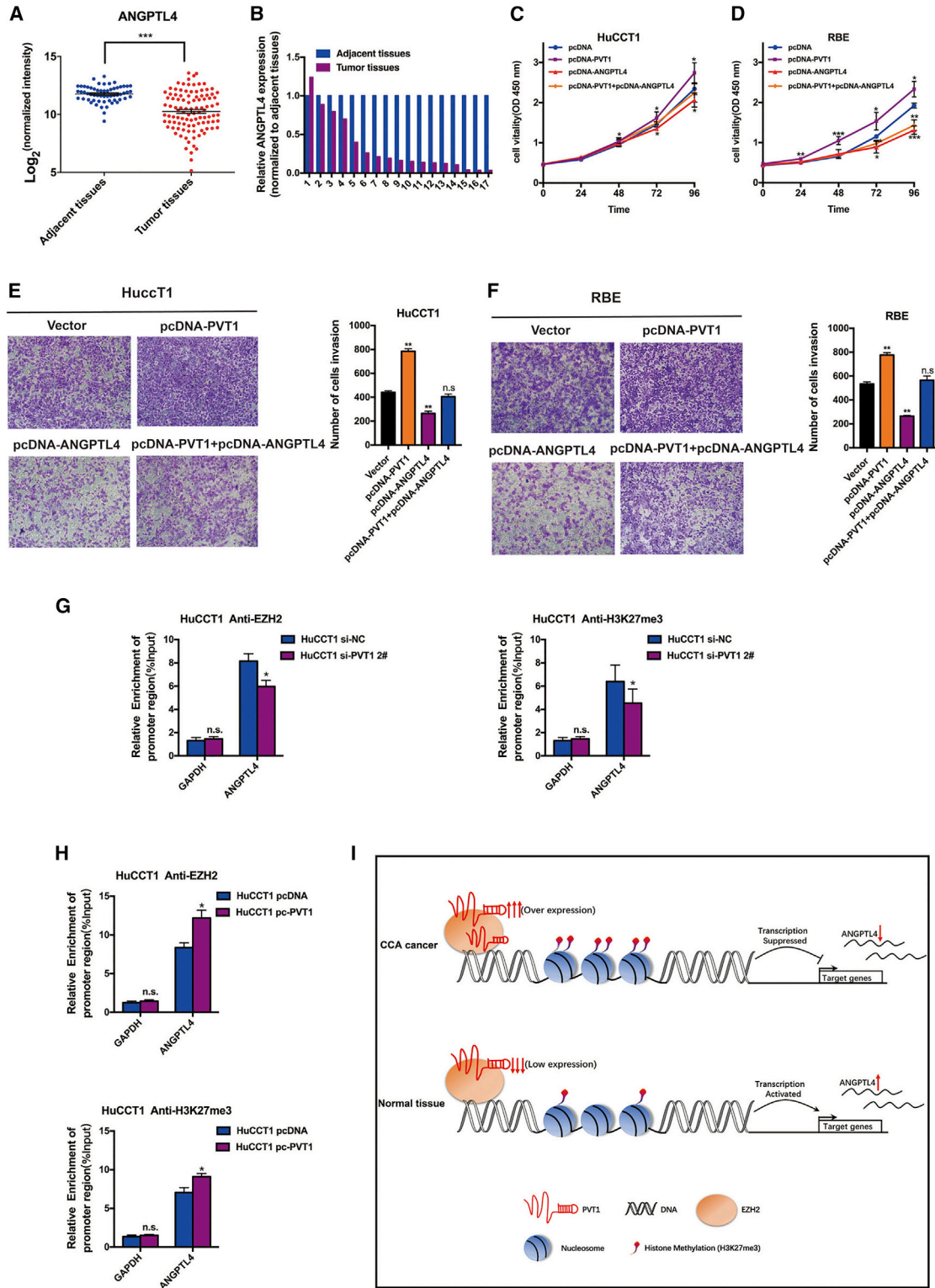
(legend on next page)

Transfection of Cell Lines

Usually, CCA cells were seeded in six-well plates and transfected with a particular siRNA (100 nM) or si-NC (100 nM) on the next day using Lipofectamine 2000 (Invitrogen), following the manufacturer's protocol (Invitrogen). The si-NC was purchased from Invitrogen (Invitrogen, CA, USA). sh-*PVT1* was cloned into the pENTR/U6 vector, and the sequences of the siRNAs and small hairpin RNA (shRNA) are summarized in Table S1.

Cell Proliferation Analysis

Cell viability was monitored with a CCK-8 (Houston, TX, USA) following the manufacturer's suggestions. HuCCT1 and RBE cells transfected with siRNA or si-negative control (NC) (3,000 cells/well) were cultivated in five 96-well plates with six replicate wells. For the colony formation assay, 500 transfected cells were combined in a six-well plate and kept in medium with 10% FBS for 2 weeks, with the replacement of medium every 4 days. Then, the colonies were confirmed with methanol and dyed with 0.1% crystal violet (Sigma-Aldrich) for 15 min. Colony formation was determined as the quantity of visibly stained colonies. Wells were measured in triplicate for the different treatment groups.

Assays of Cell Invasion

For the migration assays, after 24 hr of transfection, 3.5×10^4 cells in medium with 1% FBS were added to the upper chamber of a transwell insert (Millipore, Billerica, MA, USA), while medium with 10% FBS was added to the lower chamber. After 24 hr of incubation, the remaining cells on the upper level of the membrane were cleaned, while those cells that had migrated through the membrane were dyed with methanol and 0.1% crystal violet and then imaged with an IX71 inverted microscope (Olympus, Tokyo, Japan). The experiment was performed in triplicate.

Flow Cytometric Analysis

Flow cytometry assays were performed as previously reported by Xu et al.[45] After the cells were transfected with siRNAs for 48 hr, we harvested the cells and performed fluorescein isothiocyanate (FITC)-annexin V and propidium iodide (PI) staining using an FITC-Annexin V Apoptosis Detection Kit (BD Biosciences, Franklin Lakes, NJ, USA), according to the manufacturer's instructions. The cell cycle phase distribution was analyzed by staining with propidium oxide with a Cycletest Plus DNA Kit (BD Biosciences), following the manufacturer's instructions and evaluating the staining with a FACScan system. The percentage of cells in each phase was assessed.

Western Blot Assay and Antibodies

Cells' protein lysates were separated by 10% SDS-PAGE, transferred to 0.22-μm NC membranes (Sigma-Aldrich), and cultivated with specific antibodies. Densitometry (Quantity One software; Bio-Rad) was used to quantify the protein band density. A GAPDH antibody was employed as a control. Anti-EZH2 was obtained from Proteintech (Wuhan, China), and anti-ANGPTL4 was obtained from R&D Systems (Minneapolis, MN, USA).

In Vivo Tumor Formation Assay

The 4-week-old athymic male mice, bought from the Animal Centre of Nanjing University (Nanjing, China), were kept under specific pathogen-free conditions. HuCCT1 cells were stably transfected with shRNA or empty vector, harvested from cell culture plates, cleaned with PBS, and resuspended at a density of 2×10^7 cells/mL. Then, the cells were xenografted into BALB/c male nude mice. The sizes of the tumors were calculated every 4 days with the following equation: length $\times$ width^2 $\times$ 0.5. At 16 days post-injection, the mice were asphyxiated with CO_2, and the tumors were weighed and examined. The study was performed in strict accordance with the Guidelines for the Care and Use of Laboratory Animals of the NIH. The protocol was licensed by the Committee on the Ethics of Animal Experiments of Nanjing Medical University.

Deep Sequencing of the Whole Transcriptome

Total RNA from the HuCCT1 cells with *PVT1* knockdown and the control HuCCT1 cells was extracted and quantified. The concentration of RNA in each sample was measured with a NanoDrop 2000 (Thermo Scientific, USA), and the amount was evaluated with an Agilent 2200 system (Agilent, USA). The sequencing library of each RNA sample was prepared with an Ion Proton Total RNA-Seq Kit version (v.)2, following the protocol recommended by the manufacturer (Life Technologies, USA). The data are provided in Table S2.

Subcellular Fractionation Assay

Nuclear and cytosolic fractions were separated with a PARIS Kit (Life Technologies, Carlsbad, CA, USA), following the manufacturer's instructions.

RNA FISH

A FISH kit designed for PVT1 was purchased from RiboBio (Guangzhou, China). Briefly, cells were rinsed in PBS and then fixed in 4% formaldehyde for 10 min. Then, the RBE cells were incubated in PBS containing 0.5% Triton X-100 at 4°C for 5 min, washed with PBS three times for 5 min, and prehybridized at 37°C for 30 min.

Figure 7. *PVT1* Binds with EZH2 in the Nucleus and Epigenetically Silences *ANGPTL4*, Inhibiting Cell Proliferation and Migration in CCA Cell Lines

(A) Expression level of *ANGPTL4* in cholangiocarcinoma based on the analysis of GEO: GSE26566 data. (B) *ANGPTL4* expression was determined in 17 pairs of CCA tissues by qRT-PCR. (C–F) HuCCT1 and RBE cells transfected with vector/*ANGPTL4*/pcDNA-*PVT1* and cells transfected with *PVT1* followed by transfection with *ANGPTL4*. After transfection, the cells were analyzed by CCK-8 assays (C and D) and transwell assays (E and F). (G and H) ChIP of EZH2 and H3K27me3 of the promoter region of the *ANGPTL4* locus after siRNA treatment with si-NC and si-*PVT1* 2# (G) or overexpression of *PVT1* (H) in HuCCT1 cells. qPCR was performed to quantify the ChIP assay products. Enrichment was quantified relative to the input controls. Antibodies directed against IgG were used as a negative control. (I) Proposed model by which *PVT1* regulates *ANGPTL4* expression to promote CCA tumor growth. The error bars indicate the means ± SD. *p < 0.05, **p < 0.01, ***p < 0.001; ns, not significant.

For hybridization, anti-PVT1, anti-U6, and anti-18S oligodeoxynucleotide probes were used in hybridization solution at 37°C overnight in the dark. Subsequently, the cells were counterstained with DAPI and imaged with a confocal laser-scanning microscope (Carl Zeiss, Germany).

RIP Assays

A RIP assay was carried out to study whether *PVT1* could interact with EZH2 with a Magna RIP RNA-Binding Protein Immunoprecipitation Kit (Millipore, Billerica, MA, USA), following the manufacturer's instructions. The EZH2 antibody used for the RIP assays was obtained from Millipore (Billerica, MA, USA).

Double Fluorescence Detection of EZH2 Protein and *PVT1* mRNA in HuCCT1 Cells

HuCCT1 cells were fixed with 4% paraformaldehyde overnight, washed with PBS, and then dehydrated. After rehydration, *in situ* hybridization was performed with a fluorescein-labeled PVT1 probe (RiboBio, Guangzhou, China), followed by reaction with a goat anti-EZH2 antibody (Proteintech, Wuhan, China) at 4°C overnight. Then, the samples were counterstained with DAPI. The fluorescent signals were detected using a Zeiss LSM 700 laser-scanning microscope system (Carl Zeiss) and analyzed with ZEN lite 2.3 software (Carl Zeiss).

ChIP Assays

ChIP assays were carried out with an EZ-ChIP Kit following the manufacturer's recommendations (Millipore, USA). Antibodies against EZH2 were purchased from Millipore (Billerica, MA, USA), and antibodies against H3 trimethyl Lys27 (H3K27me3) were purchased from Abcam (Cambridge, UK). The sequences of the ChIP primers are shown in Table S1. The equation by which we calculated the ChIP signals as percentages of the input DNA was as follows: $2[\text{Input Ct} - \text{Target Ct}] \times 0.1 \times 100$.

Statistical Analysis

Statistical analyses were carried out with GraphPad Prism 5 (GraphPad, La Jolla, CA, USA). The statistical significance of the differences between various groups was calculated with Student's t tests or chi-square tests, as appropriate. All data are presented as the means ± SD. A two-sided alpha level of 0.05 was used to determine statistical significance.

SUPPLEMENTAL INFORMATION

Supplemental Information includes two tables and can be found with this article online at https://doi.org/10.1016/j.omtn.2018.10.001.

AUTHOR CONTRIBUTIONS

Conceptualization, L.M. and Y.Y.; Methodology, Y.Y. and M.Z.; Software, J.L.; Writing – Original Draft, Y.Y.; Writing – Review and Editing, L.M., J.Y., S.Y., and Q.L.; Funding Acquisition, L.M.; Resources, N.W., F.W., B.X., and X.H.; Supervision, L.M. and G.J.

CONFLICTS OF INTEREST

The authors have no conflicts of interest.

REFERENCES

1. Wang, W.T., Ye, H., Wei, P.P., Han, B.W., He, B., Chen, Z.H., and Chen, Y.Q. (2016). LncRNAs H19 and HULC, activated by oxidative stress, promote cell migration and invasion in cholangiocarcinoma through a ceRNA manner. J. Hematol. Oncol. 9, 117.

2. Rizvi, S., Borad, M.J., Patel, T., and Gores, G.J. (2014). Cholangiocarcinoma: molecular pathways and therapeutic opportunities. Semin. Liver Dis. 34, 456–464.

3. Rizvi, S., and Gores, G.J. (2017). Emerging molecular therapeutic targets for cholangiocarcinoma. J. Hepatol. 67, 632–644.

4. Rizvi, S., and Gores, G.J. (2013). Pathogenesis, diagnosis, and management of cholangiocarcinoma. Gastroenterology 145, 1215–1229.

5. Zhu, A.X. (2015). Future directions in the treatment of cholangiocarcinoma. Best Pract. Res. Clin. Gastroenterol. 29, 355–361.

6. Valle, J., Wasan, H., Palmer, D.H., Cunningham, D., Anthoney, A., Maraveyas, A., Madhusudan, S., Iveson, T., Hughes, S., Pereira, S.P., et al.; ABC-02 Trial Investigators (2010). Cisplatin plus gemcitabine versus gemcitabine for biliary tract cancer. N. Engl. J. Med. 362, 1273–1281.

7. Lee, S., Kopp, F., Chang, T.C., Sataluri, A., Chen, B., Sivakumar, S., Yu, H., Xie, Y., and Mendell, J.T. (2016). Noncoding RNA NORAD Regulates Genomic Stability by Sequestering PUMILIO Proteins. Cell 164, 69–80.

8. Niazi, F., and Valadkhan, S. (2012). Computational analysis of functional long noncoding RNAs reveals lack of peptide-coding capacity and parallels with 3′ UTRs. RNA 18, 825–843.

9. Zhao, J., Liu, Y., Zhang, W., Zhou, Z., Wu, J., Cui, P., Zhang, Y., and Huang, G. (2015). Long non-coding RNA Linc00152 is involved in cell cycle arrest, apoptosis, epithelial to mesenchymal transition, cell migration and invasion in gastric cancer. Cell Cycle 14, 3112–3123.

10. Jia, H., Osak, M., Bogu, G.K., Stanton, L.W., Johnson, R., and Lipovich, L. (2010). Genome-wide computational identification and manual annotation of human long noncoding RNA genes. RNA 16, 1478–1487.

11. Saha, A., Bhattacharya, S., and Bhattacharya, A. (2016). Serum stress responsive gene EhslncRNA of Entamoeba histolytica is a novel long noncoding RNA. Sci. Rep. 6, 27476.

12. Hu, X., Feng, Y., Zhang, D., Zhao, S.D., Hu, Z., Greshock, J., Zhang, Y., Yang, L., Zhong, X., Wang, L.P., et al. (2014). A functional genomic approach identifies FAL1 as an oncogenic long noncoding RNA that associates with BMI1 and represses p21 expression in cancer. Cancer Cell 26, 344–357.

13. Sun, M., Nie, F., Wang, Y., Zhang, Z., Hou, J., He, D., Xie, M., Xu, L., De, W., Wang, Z., and Wang, J. (2016). LncRNA HOXA11-AS Promotes Proliferation and Invasion of Gastric Cancer by Scaffolding the Chromatin Modification Factors PRC2, LSD1, and DNMT1. Cancer Res. 76, 6299–6310.

14. Guttman, M., Donaghey, J., Carey, B.W., Garber, M., Grenier, J.K., Munson, G., Young, G., Lucas, A.B., Ach, R., Bruhn, L., et al. (2011). lincRNAs act in the circuitry controlling pluripotency and differentiation. Nature 477, 295–300.

15. Atianand, M.K., Hu, W., Satpathy, A.T., Shen, Y., Ricci, E.P., Alvarez-Dominguez, J.R., Bhatta, A., Schattgen, S.A., McGowan, J.D., Blin, J., et al. (2016). A Long Noncoding RNA lincRNA-EPS Acts as a Transcriptional Brake to Restrain Inflammation. Cell 165, 1672–1685.

16. Yang, H., Liu, P., Zhang, J., Peng, X., Lu, Z., Yu, S., Meng, Y., Tong, W.M., and Chen, J. (2016). Long noncoding RNA MIR31HG exhibits oncogenic property in pancreatic

ductal adenocarcinoma and is negatively regulated by miR-193b. Oncogene *35*, 3647–3657.

17. Guttman, M., and Rinn, J.L. (2012). Modular regulatory principles of large non-coding RNAs. Nature *482*, 339–346.

18. Shi, X., Sun, M., Wu, Y., Yao, Y., Liu, H., Wu, G., Yuan, D., and Song, Y. (2015). Post-transcriptional regulation of long noncoding RNAs in cancer. Tumour Biol. *36*, 503–513.

19. Ma, S.L., Li, A.J., Hu, Z.Y., Shang, F.S., and Wu, M.C. (2015). Co-expression of the carbamoyl-phosphate synthase 1 gene and its long non-coding RNA correlates with poor prognosis of patients with intrahepatic cholangiocarcinoma. Mol. Med. Rep. *12*, 7915–7926.

20. Lu, X., Zhou, C., Li, R., Deng, Y., Zhao, L., and Zhai, W. (2017). Long Noncoding RNA AFAP1-AS1 Promoted Tumor Growth and Invasion in Cholangiocarcinoma. Cell. Physiol. Biochem. *42*, 222–230.

21. Jiang, X.M., Li, Z.L., Li, J.L., Zheng, W.Y., Li, X.H., Cui, Y.F., and Sun, D.J. (2017). LncRNA CCAT1 as the unfavorable prognostic biomarker for cholangiocarcinoma. Eur. Rev. Med. Pharmacol. Sci. *21*, 1242–1247.

22. Zhang, F., Wan, M., Xu, Y., Li, Z., Leng, K., Kang, P., Cui, Y., and Jiang, X. (2017). Long noncoding RNA PCAT1 regulates extrahepatic cholangiocarcinoma progression via the Wnt/β-catenin-signaling pathway. Biomed. Pharmacother. *94*, 55–62.

23. Tan, X., Huang, Z., and Li, X. (2017). Long Non-Coding RNA MALAT1 Interacts With miR-204 to Modulate Human Hilar Cholangiocarcinoma Proliferation, Migration, and Invasion by Targeting CXCR4. J. Cell. Biochem. *118*, 3643–3653.

24. Wang, C., Mao, Z.P., Wang, L., Wu, G.H., Zhang, F.H., Wang, D.Y., and Shi, J.L. (2017). Long non-coding RNA MALAT1 promotes cholangiocarcinoma cell proliferation and invasion by activating PI3K/Akt pathway. Neoplasma *64*, 725–731.

25. Zhang, C., Li, J.Y., Tian, F.Z., Zhao, G., Hu, H., Ma, Y.F., and Yang, Y.L. (2017). LncRNA NEAT1 Promotes Growth and Metastasis of Cholangiocarcinoma Cells. Oncol. Res. *26*, 879–888.

26. Zhang, S., Xiao, J., Chai, Y., Du, Y.Y., Liu, Z., Huang, K., Zhou, X., and Zhou, W. (2017). LncRNA-CCAT1 Promotes Migration, Invasion, and EMT in Intrahepatic Cholangiocarcinoma Through Suppressing miR-152. Dig. Dis. Sci. *62*, 3050–3058.

27. Guan, Y., Kuo, W.L., Stilwell, J.L., Takano, H., Lapuk, A.V., Fridlyand, J., Mao, J.H., Yu, M., Miller, M.A., Santos, J.L., et al. (2007). Amplification of PVT1 contributes to the pathophysiology of ovarian and breast cancer. Clin. Cancer Res. *13*, 5745–5755.

28. Li, X., Chen, W., Wang, H., Wei, Q., Ding, X., and Li, W. (2017). Amplification and the clinical significance of circulating cell-free DNA of PVT1 in breast cancer. Oncol. Rep. *38*, 465–471.

29. Li, P.D., Hu, J.L., Ma, C., Ma, H., Yao, J., Chen, L.L., Chen, J., Cheng, T.T., Yang, K.Y., Wu, G., et al. (2017). Upregulation of the long non-coding RNA PVT1 promotes esophageal squamous cell carcinoma progression by acting as a molecular sponge of miR-203 and LASP1. Oncotarget *8*, 34164–34176.

30. Tseng, Y.Y., Moriarity, B.S., Gong, W., Akiyama, R., Tiwari, A., Kawakami, H., Ronning, P., Reuland, B., Guenther, K., Beadnell, T.C., et al. (2014). PVT1 dependence in cancer with MYC copy-number increase. Nature *512*, 82–86.

31. Kong, R., Zhang, E.B., Yin, D.D., You, L.H., Xu, T.P., Chen, W.M., Xia, R., Wan, L., Sun, M., Wang, Z.X., et al. (2015). Long noncoding RNA PVT1 indicates a poor prognosis of gastric cancer and promotes cell proliferation through epigenetically regulating p15 and p16. Mol. Cancer *14*, 82.

32. Marchese, F.P., and Huarte, M. (2014). Long non-coding RNAs and chromatin modifiers: their place in the epigenetic code. Epigenetics *9*, 21–26.

33. Shen, X., Liu, Y., Hsu, Y.J., Fujiwara, Y., Kim, J., Mao, X., Yuan, G.C., and Orkin, S.H. (2008). EZH1 mediates methylation on histone H3 lysine 27 and complements EZH2 in maintaining stem cell identity and executing pluripotency. Mol. Cell *32*, 491–502.

34. Zhang, E., Han, L., Yin, D., He, X., Hong, L., Si, X., Qiu, M., Xu, T., De, W., Xu, L., et al. (2017). H3K27 acetylation activated-long non-coding RNA CCAT1 affects cell proliferation and migration by regulating SPRY4 and HOXB13 expression in esophageal squamous cell carcinoma. Nucleic Acids Res. *45*, 3086–3101.

35. Mirabello, L., Kratz, C.P., Savage, S.A., and Greene, M.H. (2012). Promoter methylation of candidate genes associated with familial testicular cancer. Int. J. Mol. Epidemiol. Genet. *3*, 213–227.

36. Wu, B.Q., Jiang, Y., Zhu, F., Sun, D.L., and He, X.Z. (2017). Long Noncoding RNA PVT1 Promotes EMT and Cell Proliferation and Migration Through Downregulating p21 in Pancreatic Cancer Cells. Technol. Cancer Res. Treat. *16*, 819–827.

37. Yan, C., Chen, Y., Kong, W., Fu, L., Liu, Y., Yao, Q., and Yuan, Y. (2017). PVT1-derived miR-1207-5p promotes breast cancer cell growth by targeting STAT6. Cancer Sci. *108*, 868–876.

38. Ding, C., Yang, Z., Lv, Z., Du, C., Xiao, H., Peng, C., Cheng, S., Xie, H., Zhou, L., Wu, J., and Zheng, S. (2015). Long non-coding RNA PVT1 is associated with tumor progression and predicts recurrence in hepatocellular carcinoma patients. Oncol. Lett. *9*, 955–963.

39. Yuan, C.L., Li, H., Zhu, L., Liu, Z., Zhou, J., and Shu, Y. (2016). Aberrant expression of long noncoding RNA PVT1 and its diagnostic and prognostic significance in patients with gastric cancer. Neoplasma *63*, 442–449.

40. Tsai, M.C., Manor, O., Wan, Y., Mosammaparast, N., Wang, J.K., Lan, F., Shi, Y., Segal, E., and Chang, H.Y. (2010). Long noncoding RNA as modular scaffold of histone modification complexes. Science *329*, 689–693.

41. Yoon, J.H., Abdelmohsen, K., Kim, J., Yang, X., Martindale, J.L., Tominaga-Yamanaka, K., White, E.J., Orjalo, A.V., Rinn, J.L., Kreft, S.G., et al. (2013). Scaffold function of long non-coding RNA HOTAIR in protein ubiquitination. Nat. Commun. *4*, 2939.

42. Puvvula, P.K., Desetty, R.D., Pineau, P., Marchio, A., Moon, A., Dejean, A., and Bischof, O. (2014). Long noncoding RNA PANDA and scaffold-attachment-factor SAFA control senescence entry and exit. Nat. Commun. *5*, 5323.

43. Okochi-Takada, E., Hattori, N., Tsukamoto, T., Miyamoto, K., Ando, T., Ito, S., Yamamura, Y., Wakabayashi, M., Nobeyama, Y., and Ushijima, T. (2014). ANGPTL4 is a secreted tumor suppressor that inhibits angiogenesis. Oncogene *33*, 2273–2278.

44. Hattori, N., Okochi-Takada, E., Kikuyama, M., Wakabayashi, M., Yamashita, S., and Ushijima, T. (2011). Methylation silencing of angiopoietin-like 4 in rat and human mammary carcinomas. Cancer Sci. *102*, 1337–1343.

45. Xu, Y., Ge, Z., Zhang, E., Zuo, Q., Huang, S., Yang, N., Wu, D., Zhang, Y., Chen, Y., Xu, H., et al. (2017). The lncRNA TUG1 modulates proliferation in trophoblast cells via epigenetic suppression of RND3. Cell Death Dis. *8*, e3104.